Above-Threshold Ionization by an Elliptically Polarized Field: Quantum Tunneling Interferences and Classical Dodging

G. G. Paulus, F. Zacher, and H. Walther*
Max-Planck-Institut für Quantenoptik, 85748 Garching, Germany

A. Lohr, W. Becker,† and M. Kleber
Physik-Department T30, Technische Universität München, 85747 Garching, Germany
(Received 11 April 1997)

Measurements of above-threshold ionization electron spectra in an elliptically polarized field as a function of the ellipticity are presented. In the rescattering regime, electron yields quickly drop with increasing ellipticity. The yields of lower-energy electrons rise again when circular polarization is approached. A classical explanation for these effects is provided. Additional local maxima in the yields of lower-energy electrons can be interpreted as being due to interferences of electron trajectories that tunnel out at different times within one cycle of the field. [S0031-9007(97)05059-X]

PACS numbers: 32.80.Rm, 03.65.Sq

The interaction of strong laser fields with matter has become a rapidly evolving discipline in recent years. One typical phenomenon is above-threshold ionization (ATI) of atoms, i.e., the absorption of more photons than necessary for ionization, leading to a series of peaks in the electron energy spectra; for a review see Ref. [1]. Above-threshold ionization spectra display various characteristic properties, such as the plateau [2] and side lobes in the angular distributions [3]. Remarkably, these and other features are qualitatively similar for different atomic systems, in particular for the rare gases. A lot of insight was gained from a classical model that treats the atom as just a source that provides electrons via tunneling [4]. Subsequently, the atomic binding potential is ignored and the electrons are described by their classical trajectories merely in the laser field. This simple picture has explained [5] both the plateau and the side lobes. Thus many strong-field effects are "universal" since they do not qualitatively depend on any particular property of the individual atom, as much as they are "classical" to the extent that they can be qualitatively explained by the just mentioned classical model.

In this Letter we report novel features in the ATI spectra generated by an elliptically polarized laser field. All of them are universal, i.e., have a similar appearance for all rare gas atoms studied, but only two of them are classical in terms of the above classification. The third effect owes its existence to a genuine quantum phenomenon: interference of electrons that reaches the continuum via tunneling at different times. The quantum interferences reported in this Letter are observed and discussed for elliptically polarized laser fields. They are, however, present for other polarizations as well, although more difficult to detect in experiments.

In addition to establishing the relevance of quantum interference to intense-field physics, this Letter presents an interesting link to other tunneling phenomena: In three-dimensional tunneling more than one most probable escape path may exist [6] and the contributions from these paths may interfere. In fact, the interference effect measured here in intense-field ionization with elliptically polarized laser light is exactly such as interference of two tunneling paths, whose experimental observation is, to our knowledge, described here for the first time. Futhermore, there is a close connection to the problem of tunneling times, in our case for a dynamic tunneling phenomenon. The theory outlined below to explain the interference effects in the ATI spectra also provides means to extract from the data complex times with an imaginary part that sets the scale for the tunneling time. ATI by an elliptically polarized field has been investigated before [7], but with different emphasis.

The experimental setup consists of a femtosecond dye laser whose pulses are brought to an energy of about 15 μJ in a two-stage optical amplifier pumped by a copper-vapor laser with a repetition rate of 6.2 kHz. The amplified pulses have a FWHM duration of 50 fs at a wavelength of 630 nm and can be focused down to 12 μm giving rise to intensities in excess of 10^{14} W/cm^2. For the analysis of the kinetic energy of the photoelectrons we use a high-resolution time-of-flight spectrometer capable of recording several electrons per laser shot with a collecting angle of 5°. The ellipticity of the laser polarization is controlled by a quarter wave plate mounted on a stepper-driven rotary stage. The big axis of the polarization ellipse always points in the direction of the electron detector. In a measurement of an ellipticity distribution, the ellipticity is scanned several times in order to minimize artifacts from possible long-term drifts in the laser intensity. The respective ATI spectra are recorded with a computer that mimics 73 different multichannel analyzers, one for each position of the quarter-wave plate. Data have been taken for all the rare gas atoms. The effects to

 0031-9007/98/80(3)/484(4)$15.00

be discussed do not qualitatively differ for the various atomic species.

We begin the discussion of the experimental results with the ellipticity distributions (EDs) of the plateau electrons for which a typical result at 32.6 eV is shown in Fig. 1. In the main part of this figure the normalized electron yield in the direction of the large axis of the polarization ellipse for energy intervals ΔE with different mean energy E is plotted versus the ellipticity of the laser polarization. We have chosen the energy intervals in accordance with the peaks of the ATI spectrum for linear polarization. This spectrum is displayed in the inset of Fig. 1. The appearance of the ED is rather simple and very similar for all energies in the plateau region: The electron yield drops very quickly for increasing ellipticity ξ; for $\xi > 0.35$ it is more than 2 orders of magnitude lower than the maximum. Note the logarithmic scale of the figures. The width of the EDs is similar for all the ATI peaks in the plateau region indicating their common origin. However, a small trend towards narrower EDs for higher electron energies is observed.

For energies below the plateau region the EDs change dramatically. The corresponding curves are in general significantly broader and for all ellipticities the electron yield is well above the detection limit; see Figs. 1 and 2. The most conspicuous effect is a local maximum in the electron yield for circular polarization, called a "wing" in Ref. [8]. Since the peak electric field strength is lower for circular polarization and since the electron has to overcome the angular momentum barrier, this is counterintuitive. The ratio of the local maximum at $\xi = 1$ and the maximum at $\xi = 0$ decreases for increasing electron energy. In the plateau region there are no electrons for $\xi = 1$. Superimposed on this general structure is another local maximum as well as one or several "shoulders," most clearly visible in Fig. 2. In contrast to the case discussed above, this whole structure moves to lower ellipticities with increasing energy. In this process, the local maximum is softened into another shoulder.

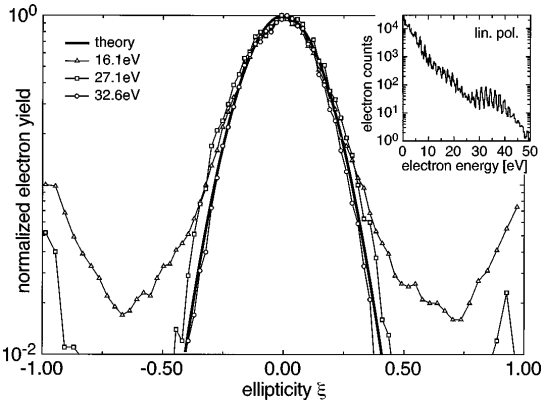

FIG. 1. Ellipticity distributions of xenon at an intensity of $\approx 0.8 \times 10^{14}$ W/cm^2. The inset displays the ATI spectrum for linear polarization.

The EDs of the plateau electrons are readily explained using the well-known rescattering model which assumes that the electron yield in the plateau is proportional to the overlap of the initial and the returning wave packet, the same mechanism that has been evoked for high-harmonic generation and nonsequential double ionization [9]. Since the dispersion relation of a wave packet is known, the only remaining parameter is its initial width a_0. In the quasistatical limit, there is a simple expression for this quantity [10]. Let us consider the electric field $\mathbf{E}(T) = E_L(\hat{\mathbf{x}} \sin \omega t - \xi \hat{\mathbf{y}} \cos \omega t)$, and let $|E_0|$ denote the ionization energy of the atom. Then, in atomic units, $a_0 = (1/(2|E_0|) + \sqrt{2|E|}/E_L)^{1/2}$. The result of this semiclassical analysis is given by the bold curve of Fig. 1 which matches the data almost perfectly. Electron yields below the plateau decrease as well with increasing ellipticity, but for a different reason. These electrons (the "direct electrons") predominantly leave the field region without rescattering. A simple analysis of the classical equations of motion shows that electrons released in the elliptically polarized field near its maximum tend to dodge the large component of the field. With increasing ellipticity they move away from the atom more and more in the direction of the small component. This also follows from an investigation [11] of the quantum mechanical expression such as Eq. (1) below. When circular polarization is approached this effect decreases as all directions become more and more equivalent, and the rates rise again. There is no reason for such a rise in the rescattering regime and, indeed, no such rise is observed.

In order to understand the moving maxima, a quantum description turns out to be necessary. The simplest known possibility is the Keldysh-Faisal-Reiss (KFR) approximation [12,13] using a zero-range potential for the atom. The results of a numerical evaluation of this model

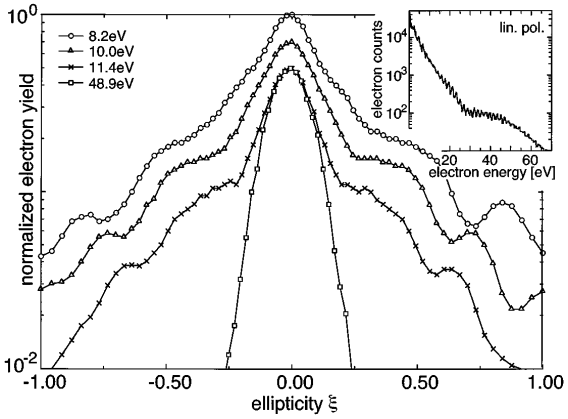

FIG. 2. Ellipticity distributions of xenon at an intensity of $\approx 1.2 \times 10^{14}$ W/cm^2. The curves are separated slightly in the vertical direction for visual convenience. They show two interference maxima moving towards linear polarization for increasing electron energy. The maxima closer to linear polarization have already merged with the global maximum for linear polarization. The inset displays the ATI spectrum for linear polarization.

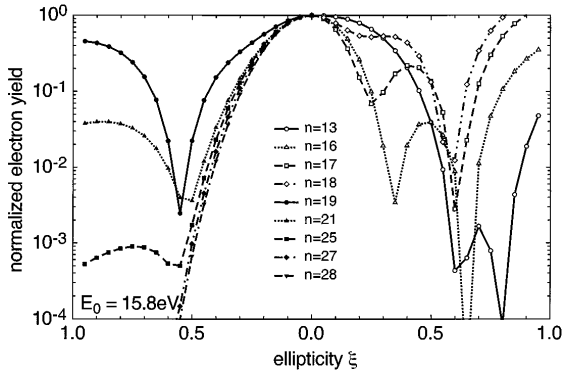

FIG. 3. ATI electron yields in the direction of the large component of the elliptically polarized driving field calculated for a zero-range atom including rescattering ($|E_0 = 15.76$ eV, $\hbar\omega = 1.96$ eV, and $U_p = 3.68$ eV). Yields are given for various energies E. The curves are labeled by the number n of photons absorbed from the ground state, $E = n\hbar\omega - |E_0| - U_p$.

augmented to include rescattering [14] are shown in Fig. 3. They nicely reproduce all of the features observed in the data, in particular the local maxima for circular polarization and the moving maxima which degenerate into a shoulder as they approach linear polarization. In order to trace these features to a quantum interference we investigate the rate of direct emission (not including rescattering).

This rate is proportional to the square of the matrix element

$$M_n = \sum_n \delta\left(\frac{\mathbf{p}^2}{2m} + |E_0| + U_p - n\omega\right) \int_0^T dt e^{iS_{\mathbf{p}}(t)}, \quad (1)$$

where the phase is just the classical action

$$S_{\mathbf{p}}(t) = |E_0|t + \int^t dt'[\mathbf{p} - e\mathbf{A}(t')]^2/2m\,. \quad (2)$$

The integral in the matrix element (1) extends over one period T of the driving laser field. The energy of the respective ATI peak is $E = n\hbar\omega - U_p - |E_0|$ where the integer n denotes the number of photons absorbed from the ground state. In agreement with the conditions of the experiment the ponderomotive potential $U_p = e^2E_L^2(1 + \xi^2)/4m\omega^2$ is kept constant while the ellipticity is varied.

If the matrix element were to describe some process having a classical limit then the integral (1) would be dominated by contributions from those times t where the action (2) is stationary, viz., $dS_{\mathbf{p}}(t)/dt = 0$. Ionization, however, involves tunneling which has no classical limit and, as a consequence, there are no real times for which the action is stationary [15]. In the spirit of the Landau-Dykhne approach to tunneling ionization [16], we make use of the fact that there are points of stationary action (saddle points) in the complex t plane, given by ($\phi_S \equiv \omega t_S$)

$$\cos\phi_S = \frac{\sqrt{1+\xi^2}}{1-\xi^2}\left\{-\sqrt{\frac{E}{2U_p}} \pm \sqrt{\frac{E}{2U_p}\,\xi^2 - \frac{|E_0|}{2U_p}(1-\xi^2) - \xi^2\frac{1-\xi^2}{1+\xi^2}}\right\}, \quad (3)$$

which, for sufficiently high intensity and energy, dominate the integral in close analogy to the classical case. Indeed, some features of the EDs can be understood just by inspection of the dependence of the saddle points on the ellipticity which is shown in the main part of Fig. 4. Let $\xi_{\max}$ denote the ellipticity for which the second square root in the parenthesis of Eq. (3) vanishes ($\xi_{\max} = 0.755$ in Fig. 4). We have to discriminate two cases: (i) For $0 \le \xi \le \xi_{\max}$, $\cos\phi_S$ is complex and there are four saddle points within the interval $0 \le \mathrm{Re}\phi_S \le 2\pi$ situated symmetrically with respect to the real axis $\mathrm{Im}\phi_S = 0$, as well as to $\mathrm{Re}\phi_S = \pi$. We may deform the contour in the integral (1) so that it passes through the two saddle points in the upper half plane at some appropriate angle. The contributions from these two saddle points interfere and the integral is approximated by [11,17] (here we are omitting some unessential factors)

$$M_n \sim \exp[\mathrm{Re}\Phi(\phi_{S1})]\cos[\mathrm{Im}\Phi(\phi_{S1}) + \psi] \quad (4)$$

with $\psi = -(1/2)\arg(\sin\phi_{S1})$ and ϕ_{S1} the saddle point with $\mathrm{Im}\phi_{S1} > 0$ and $0 < \mathrm{Re}\phi_{S1} < \pi$. (ii) On the other hand, for $\xi_{\max} \le \xi \le 1$, there are four saddle points all having $\mathrm{Re}\phi_S = \pi$ and symmetric to $\mathrm{Im}\phi_S = 0$. Now the contour is routed through the one saddle point in the upper half plane nearest the real axis and there is no interference. The corresponding approximation is just like Eq. (4), only the cosine is absent.

The two insets of Fig. 4 separately depict the squared magnitude of the two factors of Eq. (4). The left inset describes the dodging phenomenon which can be explained classically as mentioned above. For $\xi \le \xi_{\max}$, it is the cosine in Eq. (4) that is responsible for the moving maxima and the shoulders. The maxima and minima of the curve displayed in the right inset are due to constructive and destructive interference of the contributions of the two relevant saddle points (3). The ellipticities where interference is destructive are particularly well defined and can be accurately calculated by equating the cosine term to zero. They move towards linear polarization for increasing electron energy and match the minima of the numerical solution (cf. Fig. 3) very well.

The saddle points ϕ_S have an important physical interpretation as complex tunneling times [16]. The imaginary part sets the scale for the "tunneling time," i.e., the time the electron spends in the classically forbidden region. Taking

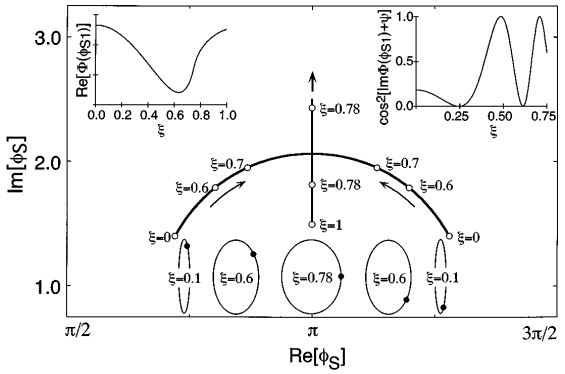

FIG. 4. Positions of the saddle points ϕ_S in the upper-half complex ϕ plane in the interval $\pi/2 \le \mathrm{Re}\phi \le 3\pi/2$, calculated from Eq. (3) for the conditions of Fig. 3 and $n = 17$. The arrows indicate the motion of the saddle points for increasing ξ. For several values of the ellipticity, insets depict the ellipse described by the electric-field vector, and the positions of the latter at the emission times $\omega t = \mathrm{Re}\phi_S$ are marked by solid dots. For $0 \le \xi < \xi_{\max}$ there are two such positions whose contributions interfere, for $\xi \ge \xi_{\max}$ there is just one corresponding to emission at $\omega t = \pi$. Emission at $\omega t = 0$ has its drift velocity in the opposite direction and does not interfere with the former. For $n = 17$, $\xi_{\max} = 0.755$. Additional insets depict, for $n = 17$, the squared magnitude and the squared cosine of the phase of the approximation (4). The ellipticities where the cosine vanishes or is maximal agree, respectively, with the minima and maxima of the ED of Fig. 3. Notice that the imaginary part of the relevant saddle point is of the order of the Keldysh parameter.

typical values for the parameters yields tunneling times of the order of a quarter of an optical cycle. The tunneling barrier, of course, is not constant at all during this interval; rather we deal with a dynamic tunneling problem. The real part can be attributed to the time at which the electron "leaves the tunnel." Thus the formal interference discussed in the preceding paragraph has physical significance: in order to reach the detector with a specific energy, for $\xi \le \xi_{\max}$ the electrons may enter the continuum at one or the other of two specific times during one optical cycle. In Fig. 4 these two times are marked by solid dots on the field ellipse; cf. the ellipses for $\xi = 0.1$ and 0.6 in the left-hand and in the right-hand part of the figure. The contributions from emission at these two times interfere. For $\xi \ge \xi_{\max}$, there is only one such and, correspondingly, no interference. In this regime, $\mathrm{Re}\phi_S = \pi$ indicating that emission occurs when the *small* component of the driving field is maximized, cf. the ellipse for $\xi = 0.78$ in Fig. 4.

Interference of different tunneling trajectories has already been conjectured to be responsible for many seemingly erratic features observed in calculations of high-harmonic generation in the context of the Lewenstein model [18].

In conclusion, we have reported several novel distinctive phenomena in ATI by elliptically polarized laser fields. The origin of one of them is interference of electrons tunneling at different times during the optical cycle. The effect is clearly visible in the experimentally observed ellipticity dependence of emission rates into individual ATI peaks. The data are qualitatively matched by calculations performed with a zero-range atom in the context of the KFR theory. This is the first time interference between different tunneling trajectories can be unambiguously identified in experimental data. Analysis of the data on the basis of the theory allows, in principle, for the determination of complex tunneling times.

This work was supported in part by Deutsche Forschungsgemeinschaft.

*Also at Sektion Physik der Ludwig-Maximilians-Universität München, Am Coulombwall 1, D-85747 Garching, Germany.

†Present address: Max-Born-Institut für Nichtlineare Optik und Kurzzeitspektroskopie, D-12474 Berlin, Germany; also at Center for Advanced Studies, Department of Physics and Astronomy, University of New Mexico, Albuquerque, NM 87131.

[1] L. F. DiMauro and P. Agostini, in *Advances in Atomic, Molecular, and Optical Physics*, edited by B. Bederson and H. Walther (Academic Press, San Diego, 1995), Vol. 35.
[2] G. G. Paulus *et al.,* Phys. Rev. Lett. **72**, 2851 (1994).
[3] B. Yang *et al.,* Phys. Rev. Lett. **71**, 3770 (1993).
[4] P. B. Corkum, Phys. Rev. Lett. **71**, 1994 (1993).
[5] G. G. Paulus *et al.,* J. Phys. B **27**, L703 (1994).
[6] T. Banks *et al.,* Phys. Rev. D **8**, 3346 (1973).
[7] M. Bashkansky *et al.,* Phys. Rev. Lett. **59**, 274 (1987); *ibid.* **60**, 2458 (1988); S. Basile *et al.,* Phys. Rev. Lett. **61**, 2435 (1988).
[8] A. Lohr *et al.,* in *Proceedings of the ICOMP96* (Institute of Physics Publishing, Bristol, Philadelphia, 1997).
[9] P. Dietrich *et al.,* Phys. Rev. A **50**, R3585 (1994).
[10] B. Gottlieb *et al.,* Phys. Rev. A **54**, R1022 (1996).
[11] S. P. Goreslavskiĭ and S. V. Popruzhenko, Zh. Eksp. Teor. Fiz. **110**, 1200 (1996) [JETP Lett. **38**, 661 (1996)]; the authors also perform a saddle point analysis of the direct emission rate for a general elliptically polarized field, but do not consider interference of different saddle points.
[12] L. V. Keldysh, Zh. Eksp. Teor. Fiz. **47**, 1945 (1964) [Sov. Phys. JETP **20**, 1307 (1964)]; F. H. M. Faisal, J. Phys. B **6**, L89 (1973).
[13] H. R. Reiss, Phys. Rev. A **22**, 1786 (1980).
[14] A. Lohr *et al.,* Phys. Rev. A **55**, R4003 (1997).
[15] M. Lewenstein *et al.,* Phys. Rev. A **51**, 1495 (1995).
[16] N. B. Delone and V. P. Krainov, *Multiphoton Processes in Atoms* (Springer-Verlag, Berlin, 1994); for a review of the concept of the tunneling time in constant fields, see E. H. Hauge and J. A. Støvneng, Rev. Mod. Phys. **59**, 917 (1989).
[17] The result (4) can be very easily obtained by proceeding just as if the saddle points were real. A rigorous evaluation has been given by C. Leubner, Phys. Rev. A **23**, 2877 (1981); similar results can also be found in Ref. [13].
[18] M. Lewenstein *et al.,* Phys. Rev. A **49**, 2117 (1994); Phys. Rev. A **52**, 4747 (1995).